Ultrasonic Studies of a Single Crystalline La_<1.85>Sr_<0.15>CuO_4 in High Magnetic Fields(Transport and Fermiology)

Ultrasonic Studies of a Single Crystalline $La_{1.85}Sr_{0.15}CuO_4$ in High Magnetic Fields *

Tetsuo Hanaguri[a], Tetsuo Fukase[a], Isao Tanaka[b] and Hironao Kojima[b]
[a]Institute for Materials Research, Tohoku University, Sendai 980, Japan
[b]Institute of Inorganic Synthesis, Yamanashi University, Kofu 400, Japan
(Received March 12, 1993)

Synopsis

Temperature dependence of the sound velocity of a single crystalline $La_{1.85}Sr_{0.15}CuO_4$ has been measured in high magnetic fields. An increase of the sound velocity due to the flux line lattice (FLL) pinning is observed at a temperature below the superconducting transition temperature T_C. Anisotropic activation energies to depin flux lines are evaluated separately from measurements under various settings of the directions of wave vector $\boldsymbol{k}$, polarization vector $\boldsymbol{u}$ and magnetic fields $\boldsymbol{H}$ using the analysis based on the thermally assisted flux flow model. Besides the FLL elasticity, anomalous temperature dependence of elastic constants of c_{33} and $(c_{11}-c_{12})/2$ (softening at low temperatures and hardening at lower temperatures below 10K) is observed in high magnetic fields.

I. Introduction

Ultrasonic measurement has been one of useful tools to investigate not only lattice properties but also electrical or superconducting properties of high-T_C oxide superconductors (HTSC). Some characteristics of HTSC, a short coherence length and a layer structure, for example, make their mixed states distinctive. Because of the short coherence lengths, the pinning energy in HTSC is relatively small and flux lines are easily depinned by small driving forces with assistance of the thermal energy. Some characteristic phenomena in HTSC, such as the large relaxation of the magnetization[1] and the broadening of the resistive transition in magnetic fields[2], are considered to be closely related to the thermally activated motion of flux lines. Tachiki and Takahashi proposed the intrinsic pinning mechanism based on the layer structure[3,4]. They have pointed out that the layer structure brings the spatial variation of the order parameter along the c-axis and flux lines which lie in the c-plane are naturally pinned at the position where the order parameter is smallest. Therefore, it is important to examine the anisotropy of the flux pinning to under-

---

* The 1940th report of Institute for Materials Research

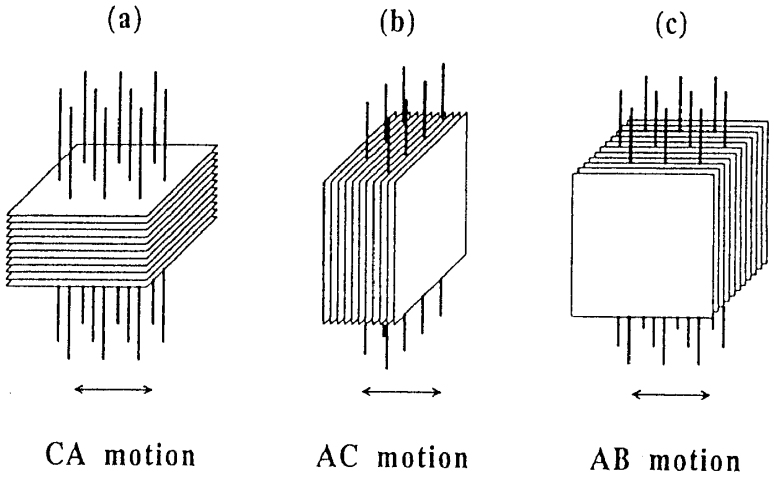

Fig. 1. Schematic illustration of three patterns of flux motions in HTSC. Lines and planes indicate flux lines and the stack of the CuO_2 planes, respectively. Arrows indicate directions of flux motions.

stand the effective pinning mechanism in HTSC.

If the uniaxial anisotropy is assumed in HTSC, there are three independent directions of flux motions as illustrated in Fig.1. For magnetic fields applied along *c*-axis, the direction of the flux motion is perpendicular to the *c*-axis (Fig.1(a)). For magnetic fields applied perpendicular to the *c*-axis, two independent directions of flux motions are possible. One of those is parallel to the *c*-axis (Fig.1(b)) and the other is perpendicular to both applied fields and the *c*-axis (Fig.1(c)). Hereafter, patterns of motions Fig.1(a),(b) and (c) are referred as the CA motion, the AC motion and the AB motion, respectively. The AC motion is related to the intrinsic pinning.

The sound velocity depends on only the elastic constant of the crystal lattice (CL) c^c_{ij} at a temperature above the depinning temperature T_p, because flux line lattice (FLL) and CL are well separated each other. At temperatures below T_p where FLL is pinned to CL, the sound velocity depends on the sum of the elastic constants of FLL c^c_{ij} and CL c^f_{ij}. Therefore, a step and a peak are observed in temperature dependence of the sound velocity and attenuation, respectively. The shape of the step and the peak depend on the activation energy to depin *U(T,H)*. Since sound waves are polarized, not only the anisotropy of flux pinning energies but also various kinds of elastic constants can be observed in our measurement, if the experiment is performed on a single crystal. Furthermore, since the ultrasonic measurement is a bulk sensitive technique, contributions from minor but strong pinning centers (e.g. domain boundaries) can be neglected. In spite of these many advan-

tages, ultrasonic experiments for this purpose have been performed only on polycrystalline samples [5,6,7].

On the other hand, elastic properties of HTSC in the superconducting and the normal states at low temperatures are not so simple as to those of usual superconductors. Ultrasonic measurements under high magnetic fields are useful to know the properties in the normal conducting state at low temperatures below $T_C(0)$ and to extract superconducting properties of HTSC. In this paper, we report ultrasonic investigations of a single crystalline $La_{1.85}Sr_{0.15}CuO_4$ under high magnetic fields up to 23 tesla.

II. Experimental

A large and high quality single crystal of $La_{1.85}Sr_{0.15}CuO_4$ was grown by the traveling solvent floating zone technique [8]. For ultrasonic measurements, the grown crystal was cut into rectangular shape in which two planes are perpendicular to the $[100]_t$ axis and $[001]_t$ axis. Each pair of planes are polished carefully to be parallel and flat. The dimensions of the sample are 4.501mm along the $[100]_t$ axis and 4.146mm along the $[001]_t$ axis. Sound waves were generated by $LiNbO_3$ transducers glued on polished planes by RTV (Shinetsu Silicone KE347W). The z-cut one was used for longitudinal waves and the x-cut one was used for transverse waves. Temperature dependence of the sound velocity V_S and attenuation α were simultaneously measured by the phase comparison method and the pulse echo method, respectively. The absolute value of V_S was determined by the pulse superposition method at 4.2K. The measuring frequencies were 21.7MHz for the longitudinal c^c_{11} mode and 23.3MHz and 23.7MHz for the transverse c^c_{44} mode.

Magnetic fields were generated by superconducting magnets up to 15 tesla and by hybrid magnets (HM-1a and HM-2 in High Field Laboratory for Superconducting Materials of IMR) up to 23 tesla. Temperature was monitored by a carbon glass thermometer of which the magnetoresistance error had been already corrected. All of the data were taken in the warming process after field cooling. Superconducting transition temperature T_C was determined as 33.5±3K by the previous measurement of V_S in the c^c_{33} mode in which V_S exhibits a clear jump at T_C [9].

III. Results

Figure 2 shows temperature dependence of the sound velocity V_S in the c^c_{11} mode measured under two kinds of settings of $\boldsymbol{k}$, $\boldsymbol{u}$ and $\boldsymbol{H}$. In this mode, V_S exhibits a clear kink at T_C and increases below T_C in the absence of magnetic fields. In the magnetic field applied perpendicular to $\boldsymbol{u}$, V_S increases in the low temperature region and is reduced in the vicinity of T_C as shown in Fig.2(a). This feature is considered to be the superposition of two effects, namely the enhancement due to the FLL elasticity and the reduction due to the

destruction of superconductivity.The pattern of the flux motion in this configuration corresponds to the AB motion and the elastic constant of FLL is c^f_{11} (compression modulus). To evaluate the influence of the destruction of superconductivity in the c^c_{11} mode, V_S was measured in the parallel configuration of the magnetic field to $\boldsymbol{u}$ in which the FLL does not couple with sound waves. The results are shown in Fig.2(b). In this configuration, the enhancement of the sound velocity below T_c monotonically decreases with increasing magnetic field. Below about 10K, magnetic fields bring little effects on V_S[10]. The origins of these phenomena are indistinct. Nevertheless, results in this configuration can be used as the backgrounds to extract the FLL elasticity with comparing to the results in the configuration of Fig.2(a).

In the case of the c^c_{44} mode, V_S is a structureless function of the temperature with barely no change at T_C in the absence of magnetic fields. Therefore, it seems that the strain e_{yz} which corresponds to the c^c_{44} mode hardly couples to superconductivity. It is expected that there are little magnetic field effect on c^c and α^c in the c^c_{44} mode. Actually, we can hardly detect any magnetic field dependence in V_S and α in the magnetic field parallel to $\boldsymbol{u}$. On the other hand, in the magnetic field perpendicular to $\boldsymbol{u}$, V_S increases by a certain

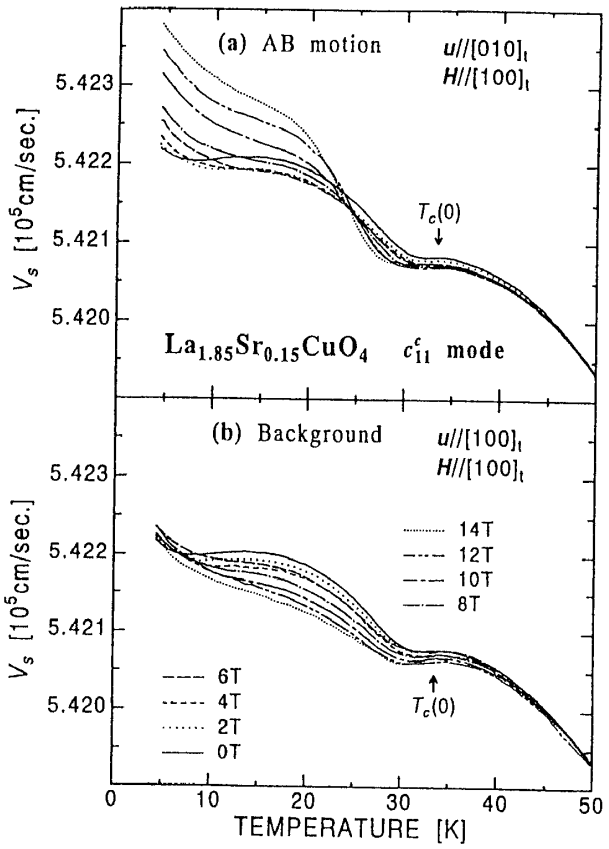

Fig. 2. Temperature dependence of the sound velocity V_S in the c^c_{11} mode under various magnetic fields. In the configuration of Fig. 2(a), FLL couples with sound waves. In the configuration of Fig. 2(b), FLL does not couple with sound waves.

fraction at a temperature below T_C. In these configurations, sound waves can couple to FLL and flux lines move as the AC motion ($\boldsymbol{k}$//[100]$_t$, $\boldsymbol{u}$//[001]$_t$, $\boldsymbol{H}$//[100]$_t$) and the CA motion ($\boldsymbol{k}$//[001]$_t$, $\boldsymbol{u}$//[100]$_t$, $\boldsymbol{H}$//[001]$_t$). Elastic constants of FLL are c^f_{44} (tilt modulus) in both configurations. We can regard that the increase of V_S in the magnetic field perpendicular to $\boldsymbol{u}$ in the c^c_{44} mode is purely due to the FLL elasticity and the pinning of FLL.

FLL contributions to V_S can be extracted for all patterns of flux motions shown in Fig.1.Temperature dependence of excess elastic constants Δc^fs induced by FLL are shown in Fig.3. The value of the mass density ρ=6.99 g/cm^3 was used to convert V_S to elastic constants using $c=\rho V_s^2$. Figures 3(a), (b) and (c) correspond to the flux motion of CA,AC and AB, respectively. In each case, Δc^f exhibits a step like increase at the temperature below T_C.

Figure 4 shows the temperature dependence of the sound velocity of the $(c^c_{11} - c^c_{12})/2$ mode ($\boldsymbol{k}$ // [110]$_t$, $\boldsymbol{u}$//[1 1 0]$_t$, $\boldsymbol{H}$ // [001]$_t$). The kink at T_c shifts to the lower temperature side and becomes indistinct with increasing magnetic field. In high magnetic fields above 6

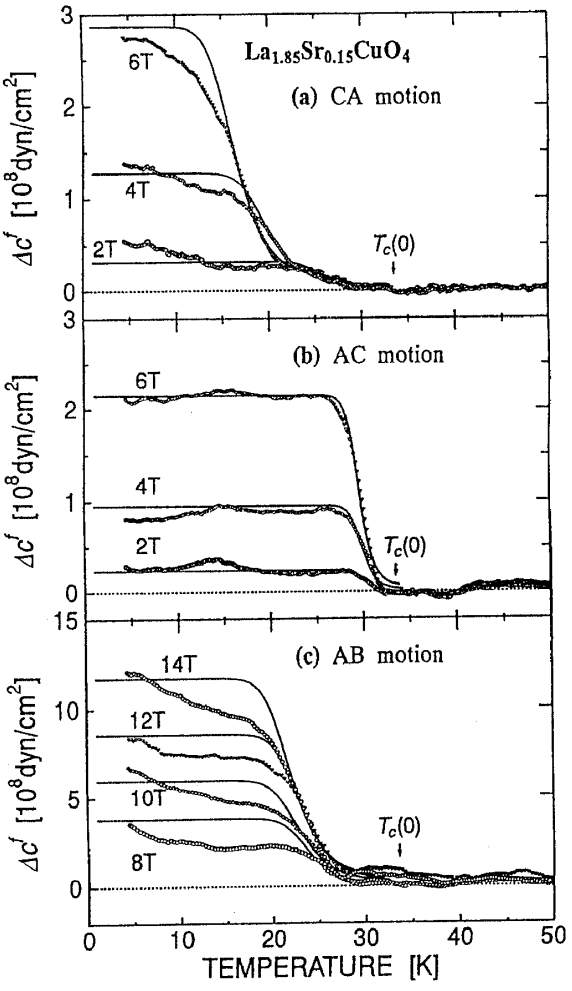

Fig. 3. Temperature dependence of the FLL induced excess elastic constant Δc^f for three patterns of flux motions illustrated in Fig. 1. Open circles indicate experimental data and solid curves are fitted ones using eqs. (1),(2),(3), (4) and the exponent n =1.5. Arrows indicate $T_C(0)$. The parameters used in fitting are listed in Table 1.

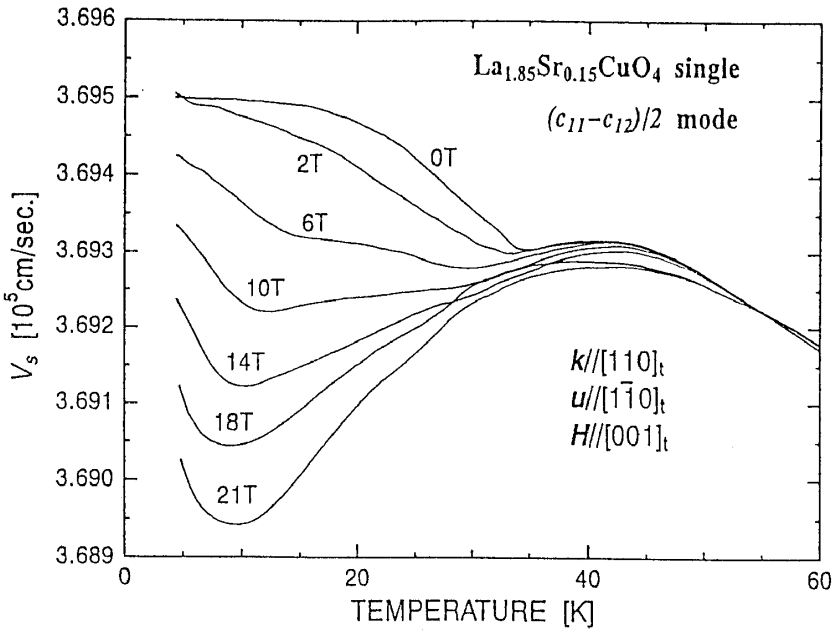

Fig. 4. Temperature dependence of the sound velocity V_S of the $(c_{11} - c_{12})/2$ mode under various magnetic fields.

tesla, another dip appears near 10K and shifts to the lower temperature side with increasing magnetic field. The softening of this mode becomes remarkable under higher magnetic fields. The dip temperature seems to locate near the irreversibility line. Although, increase of V_s due to c^f_{66} of FLL is expected in this configuration, the amount of increase of V_s below the dip temperature is extraordinarily large to compare with the expected value from c^f_{66}. Similar behavior is seen for c_{33} mode ($\boldsymbol{k}$ // $\boldsymbol{u}$// $\boldsymbol{H}$ // $[001]_t$), where the elasticity of FLL does not couple with sound waves.

IV. Discussions

First, we discuss about the temperature dependence of Δc^f. Pinning energies can be obtained to fit the data of Fig.3 to following equations (1), (2) and (3).

$$\Delta c^f = c^f_{ii} \frac{\omega^2}{\omega^2 + (c^f_{ii}\Gamma k^2)^2} \tag{1}$$

Here, ω is the angular frequency of the ultrasound and Γ is the phenomenological relaxation coefficient which represents the interaction between FLL and CL. Within the framework of the thermally assisted flux flow model,[10] Γ is related to the dc resistivity σ^{-1} caused by the flux motion with relation of

$$\sigma^{-1} = \Gamma \frac{4\pi}{c^2} \frac{H}{B} c_{44}^f \tag{2}$$

where c is the light velocity. The activation energy to depin flux lines U is related to σ^{-1} by the following Arrhenius-like formula.

$$\sigma^{-1} = \rho_0 \exp(-\frac{U}{k_B T}) \tag{3}$$

Here, ρ_0 is the proportional coefficient and k_B is the Boltzmann constant. Equations (2) and (3) represent a relation between Γ and U. Since the coefficient Γ should be different in each direction of the flux motion displayed in Fig.1, the anisotropy of U can be obtained from ultrasonic experiments under various directions of $\boldsymbol{u}$. We define U_{ca}, U_{ac} and U_{ab} which correspond to the FLL motions of CA, AC and AB, respectively. In general, both ρ_0 and U are field and temperature dependent. To analyze the resistivity, the sound velocity and attenuation, field and temperature dependence of ρ_0 and U should be suitably assumed. We adopt the model in which ρ_0 is temperature independent. Temperature dependence of U is assumed as follows.

$$U(T,H) = U(0,H) \times (1\text{-}T/T_c(H))^n \tag{4}$$

Field dependence of ρ_0 and U can be deduced to fit the data taken under various magnetic fields to eq.(1) with eqs.(2), (3) and (4). To estimate the exponent n, we first analyzed the resistivity data for each pattern of the flux motion. The low resistivity regions of the data are well expressed if n is assumed as 1.5. With using exponent n=1.5 and varying U and ρ_0, temperature dependence of Δc^f was fitted. Typical fitted curves with the experimental data are shown in Fig.3 with solid lines. In the case of the AC motion, experimental results are well fitted by eq.(1) as shown in Fig.3(b). In other cases, although eq. (1) holds well in the high temperature regions, experimental results become to deviate from the calculated curves in the low temperature regions as shown in Fig.3(a) and (c). These deviations are hardly considered to be due to the wrong choice of the temperature dependence of the pinning energies. Because these deviations still remain if U is assumed to be temperature independent (namely n=0). Since experimental data deviate *below* the calculated curve, U must *decrease* with decreasing temperature if the origin of this deviation is the temperature dependence of U. Such temperature dependence of U is unreasonable because U is considered to be proportional to the condensation energy which increases with decreasing temperature.

Table 1. The fitted results of ρ_0 and $U_{ij}(0,H)$ deduced from the sound velocity data taken under various magnetic fields.

	CA motion			AC motion			AB motion			
H(T)	2	4	6	2	4	6	8	10	12	14
ρ_0 (10^{-5} Ωcm)	3.5	3.3	3.6	10.9	4.6	4.1	14	11	11	11
$U(0,H)$ (10^2 K)	4.2	1.5	0.93	15	12	11	2.7	2.1	2.3	2.0

The parameters used in fitting are listed in Table 1. Activation energies U_{ij}'s decrease with increasing field. To fit the data with n=0 (simple Arrhenius formula) was also possible as in the case of n=1.5, and it was difficult to determine the value of n from ultrasonic data only. Activation energies in the case of n=0 are 71K at 6 tesla in the CA motion, 537K at 6 tesla in the AC motion and 132K at 14 tesla in the AB motion. The calculated activation energies are not different so much in both assumptions of n.

Next, we discuss about the anisotropy of activation energies. In the case of the ultrasonic measurement, U_{ac} is extraordinarily large among U's. Therefore, it seems that the intrinsic pinning mechanism works well, while in the case of the resistivity measurement, $U_{ac} \sim U_{ab} \gg U_{ca}$ and U's are larger than those deduced from the ultrasonic measurement. This result implies that the intrinsic pinning mechanism is not dominant for the resistivity measurement and both U_{ac} and U_{ab} are determined by some strong but minor pinning centers. The anisotropy between U_{ca} and U_{ab} is considered to be due to the anisotropy of the effective pinning center itself. In the case of the $YBa_2Cu_3O_7$ system, it is considered that twin planes act as the effective pinning center[11]. In $La_{1.85}Sr_{0.15}CuO_4$, since twin planes are parallel to the $(100)_t$ plane[12], they can contribute to both U_{ca} and U_{ab}. For the purpose of making clear the role of twin planes, the measurement of $(c^c_{11} - c^c_{12})/2$ mode will be meaningful. Comparing the two sets of results in $\boldsymbol{H}//[110]_t$ and in $\boldsymbol{H}//[1\,1\,0]_t$, the FLL contribution can be extracted by the same process which is mentioned before. In this case, since the direction of FLL motion is not perpendicular to twin planes, the value of U_{ab} which does not include the effect of twin planes can be estimated.

Finally, we discuss the peculiar temperature dependence of V_s in very high magnetic fields shown in Fig.4. The decrease of V_s in magnetic fields seems to originate in the recovery of the lattice softening suppressed by the transition to the superconducting state as the case of V_3Si[13]. The upturn of V_s seems to occur at the superconducting transition temperature T_{c2} in the case of V_3Si. In the present case it seems to occur near the irreversibility temperature. If we assume that the lattice softening is due to the band Jahn-Teller effect like the case of A15 compounds and we assume a strain sensitive narrow band at

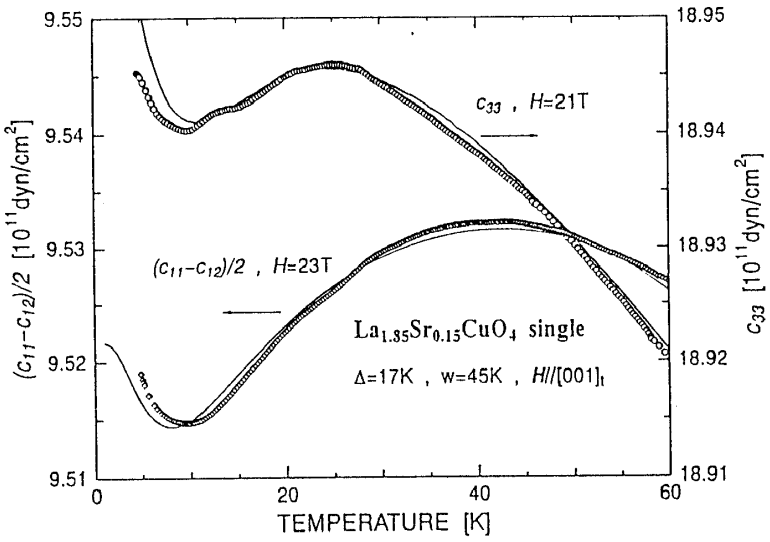

Fig. 5. Temperature dependence of the elastic constants of c_{33} *and* $(c_{11} - c_{12})/2$ under high magnetic fields. Open circles indicate experimental data and solid curves are fitted ones using eqs. (5). The parameters used in fitting are listed in the figure.

the Fermi level, we can reproduce the peculiar temperature dependence of V_s using the following equation.

$$c_{ij} = c_{ij}^0 + a^2 \int \frac{\partial f}{\partial E} D(E) dE, \tag{5}$$

where f is the Fermi function, D is the density of state of the narrow band and a is the coupling constant between the strain and the band. The fitted curves are shown in Fig.5 by solid lines. The parameters used in fitting are as follows. The band width w is 45K, the location of the center of the band below the Fermi level Δ is 17K and coupling parameter a^2D is 0.11×10^{11}dyn/cm^2 for the $(c_{11} - c_{12})/2$ mode and 0.23×10^{11}dyn/cm^2 for the c_{33} mode, respectively. However, the experimental results are well fitted by this band Jahn-Teller model, there is no evidence of such a narrow band now, experimentally and theoretically. It is necessary to test this model from other experiments, for example, specific heat measurements in high magnetic fields.

In summary, the FLL elasticity and its anisotropic pinning have been investigated in a single crystalline $La_{1.85}Sr_{0.15}CuO_4$ by ultrasonic measurements. This method is real bulk sensitive measurement and useful to investigate the anisotropy of FLL. Temperature dependence of the FLL induced excess elastic constant was explained by the model based on the thermally assisted flux flow. Three independent pinning energies U_{ca}, U_{ac} and U_{ab} were evaluated separately. It is found that $U_{ac} \gg U_{ab} > U_{ca}$. The result is consistent with the

intrinsic pinning mechanism. Besides the FLL elasticity, anomalous temperature dependence of elastic constants of c_{33} and $(c_{11}-c_{12})/2$ (softening at low temperatures and hardening at lower temperatures below 10K) was observed in high magnetic fields. The band Jahn-Teller model was proposed to explain this anomalous temperature dependence.

Acknowledgments

The authors would like to thank to Prof. T. Matsushita and Prof. N. Kobayashi for variable discussions and comments. They are also grateful to the staffs of High Field Laboratory for Superconducting Materials of IMR and the Cryogenic Center of Tohoku University for the use of the high magnetic field facilities. This work is partially supported by the Grant-in-Aid for Scientific Research on Priority Areas, "Mechanism of Superconductivity" and "Science of High T_C Superconductivity" from the Ministry of Education, Science and Culture of Japan. One of the authors (T.H.) wish to thank to the JSPS Fellowships for Japanese Junior Scientists for the financial support.

References

1) Y. Yeshurun and A. P. Malozemoff, Phys. Rev. Lett., 60 (1988) 2202.
2) T. T. M. Palstra, B. Batlogg, L. F. Schneemeyer, and J. V. Waszczak, Phys. Rev. Lett., 61 (1988) 1662.
3) M. Tachiki and S. Takahashi, Solid State Commun., 70 (1989) 291.
4) M. Tachiki and S. Takahashi, Solid State Commun., 72 (1989) 1083.
5) J. Pankert, Physica, B165&166, (1990) 1272.
6) P. Lemmens, P. Frönig, S. Ewert, J. Pankert, G. Marbach, and A. Comberg, Physica, C174 (1991) 289.
7) Y. Horie, T. Miyazaki, and T. Fukami, Physica , C175 (1991) 93.
8) I. Tanaka, K. Yamane, and H. Kojima, J. Crystal Growth, 96 (1989) 711.
9) T. Hanaguri, R. Toda, T. Fukase, I. Tanaka, and H. Kojima, Physica, C185-189 (1991) 1395.
10) J. Pankert, Physica, C168, (1990) 335.
11) W. K. Kwok, U. Welp, G. W. Crabtree, K. G. Vandervoort, R. Hulscher, and J. Z. Liu, Phys. Rev. Lett., 64 (1990) 966.
12) T. Onozuka, M. Omori, M. Hirabayashi, and Y. Syono, Jpn. J. Appl. Phys., 26 (1987) 1714.
13) N. Toyota, T. Kobayashi, M. Kataoka, H. Watanabe, T. Fukase and Y. Muto, J. Phys., Soc. Jpn., 57 (1988) 3089.